Volume 4, Issue 3, 2015, 301-305 ISSN 2284-6808

Letters in Applied NanoBioScience

www.NanoBioLetters.com

Original Research Article Open Access Journal

Received: 25.02.2015 / Revised: 15.06.2015 / Accepted: 13.09.2015/ Published on-line: 29.09.2015

Quantitative measurement of the interface adhesion of a multifunctional coating

Luciano Oliveira Castro Lara[1*], José Daniel Biasoli De Mello [1]**

[1]Laboratório de Tribologia e Materiais, Universidade Federal de Uberlândia, Uberlandia, MG, Brazil, ***ltm-demello@ufu.br***

[*]Present adress: Departamento de Engenharia Mecânica, Universidade Federal do Espírito Santo, Vitória, ES, Brazil, ***lucianocastrolara@gmail.com***

corresponding author e-mail address: ***ltm-demello@ufu.br*

ABSTRACT

Multifunctional coatings, widely used in tribological applications, have properties that are strongly influenced by the interaction of the system coating and substrate. The adhesion between the adjacent layers in a multifunctional coating is extremely important to the desired performance. This paper used equations of fracture mechanics to quantitatively measure the interface adhesion of CrN/Si-DLC coatings with different thicknesses deposited on a steel substrate (AISI 1020) by Plasma Enhanced Magnetron Sputtering (PEMS), to evaluate the influence of the thickness of the layers on the interface adhesion of the multifunctional coatings. The known critical stresses at the interface between the CrN and the DLC coatings were compared to the interface shear stresses simulated using FilmDoctor® software. The evaluation of the interface adhesion of multifunctional coatings with different layer thicknesses resulted in a design of coating systems optimised for improved durability.

Keywords: *interface adhesion, multifunctional coatings, Plasma Enhanced Magnetron Sputtering, critical stresses.*

1. INTRODUCTION

With considerable research and development, solid lubricant coatings have received significant attention from the academic and industrial communities in recent years. Despite this, no solid lubricant provides low friction and low wear under varying conditions of temperature and the environment [1]. To achieve a combination of high wear resistance, high load support and low friction, a multifunctional surface engineering process combining purpose-oriented layers can be applied [2]. This process combines the features of the multifunctional coating and the substrate.

The mechanical, thermal, electrical, optical, and other performance properties of a particular film are strongly influenced by the interaction of the system coating and substrate, thus delimiting the potential technological applications of the coating. The study of multifunctional coatings is an area of research that has grown, leading to numerous publications and suggesting that multilayer coatings have potential for tribological applications [3]. The performance of the system coating/substrate depends on the coating properties and the compromise between the properties of the system. The coating thickness strongly influences the properties of the system.

New techniques for characterising mechanical properties of materials have emerged, such as indentation. During an indentation test, spalling is induced by compressive radial stresses that are generated when a rigid indenter penetrates the coating.

Adhesion is a primary property that a multilayer coating must have for tribological applications. According to Zaidi et al. [4], insufficient adhesion can lead to premature failure due to interfacial fracture. To evaluate this property, the indentation test is widely used.

In this paper the determination of the critical stresses at the interface between CrN and DLC (interface critical stress) were made through indentation tests. In order to analyse the effect of film thickness on stress distributions on the coated systems, the results from the indentation tests were compared to the shear stresses at the simulated interfaces (interface shear stress). The simulation tests used the commercial software FilmDoctor®.

This software, which uses a Hertzian model extended to multi-layered surfaces [5-7], was developed to simulate contact and is very flexible in terms of contact geometry and loading conditions. The concept of an effective indenter, introduced by Pharr and Oliver [8], is employed in the calculations to produce the complete stress distribution for the contact under investigation [5].

2. EXPERIMENTAL DETAILS

2.1. Materials.

In this work, a thick intermediate CrN layer between the DLC coating and the substrate was designed to improve the load support of a soft AISI 1020 steel substrate. Therefore, CrN-DLC multifunctional coatings were deposited on soft AISI 1020 carbon steel substrates (HV = 120) using a proprietary Plasma Enhanced Magnetron Sputtering method. The thicknesses of both layers were varied within the range of the equipment to analyse the effects of the layer thicknesses on their tribological performance. The manipulation of the processing parameters to vary the thicknesses of the coatings produced coated specimens that could be grouped in two families of coatings, one with thicker coatings

(Family 1) and one with thinner coatings (Family 2), as shown in Fig. 1.

Three specimens with different thicknesses of DLC and CrN layers were investigated, as described in Table 1.

Table 1. Average thickness of the Si-DLC and CrN layers.

Sample	Si-DLC		CrN	
	Thickness (μm)	E (GPa)	Thickness (μm)	E (GPa)
A	1.78±0.07	105.12	3.19±0.05	84.31
B	1.53±0.05	81.82	3.49±0.09	75.43
C	1.23±0.05	203.20	1.38±0.05	235.98

This table also shows the values of Young´s modulus for each layer, obtained from instrumented indentation tests using a Vickers indenter and a normal load of 20 mN [9-10]. Young´s moduli for the Si-DLC layers were calculated from the unloading curves using the method by Oliver and Pharr [11], whereas Young´s moduli for the CrN layers were calculated using a tool for the adjustment of Young´s modulus in multi-layered coatings present in the FilmDoctor® software [12].

2.2. Measurement of interface adhesion.

Indentation testing involving significant plastic deformation in the substrate has been successfully used to quantitatively measure the adhesion of a hard coating on a ductile substrate. [13].

As shown in Fig. 2, the indentation made by an axisymmetric indenter induced interface annular cracks that spread outward radially to the point r=R.

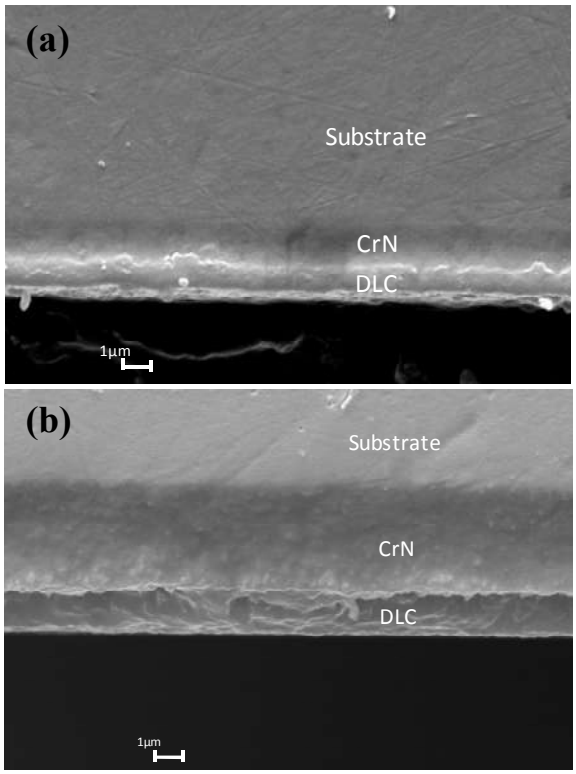

Figure 1. Cross sections of the coated systems:(a) Family 2; (b) Family 1.

As shown in Fig. 2, the indentation made by an axisymmetric indenter induced interface annular cracks that spread outward radially to the point r=R. During an indentation test, spalling can be induced by compressive radial stresses that are generated when a rigid indenter penetrates the coating [14]. During indentation, a crack propagates radially to release the elastic deformation energy stored in the coating.

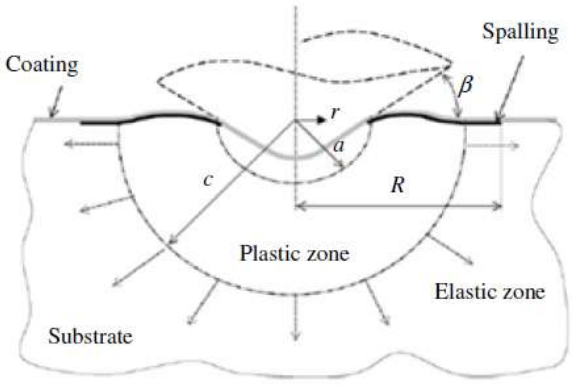

Figure 2. Schematic indentation by an axisymmetric indenter [14].

According to Drory and Hutchinson [15], the rate of energy release Gt ahead of the crack is given by:

$$G_t = \frac{\left(1-\upsilon_f^2\right)e}{2E_f}\left[\sigma_r\left(R\right)-\sigma_r\left(R^-\right)\right]^2 \quad (1)$$

Where υ_f, E_f and e are the Poisson coefficient, Young´s modulus and the thickness of the coating, respectively, and $\sigma_r(R)$ and $\sigma_r(R-)$ are the components of the radial stress on the coating within and outside the spalling region, respectively. The elastic deformation energy stored in the coating is released via spalling and therefore the interface adhesion Γc equals the energy release rate:

The radial stress outside the spalling region, $\sigma_r(R)$, is given by the generalised Hook´s law (Eq. 3). The radial stress within the spalling region, $\sigma_r(R-)$, can be given by Eq. 4 [15]:

$$\Gamma_c = G_t = \frac{\left(1-\upsilon_f^2\right)e}{2E_f}\left[\sigma_r\left(R\right)-\sigma_r\left(R^-\right)\right]^2 \quad (2)$$

$$\sigma_r\left(R\right) = \frac{E_c}{1-\upsilon_c^2}\left[\varepsilon_r\left(R\right)+\upsilon\varepsilon_\theta\left(R\right)\right] \quad (3)$$

$$\sigma_r\left(R^-\right) = -\frac{E_c\varepsilon_\theta\left(R\right)\left[1-\left(a/R\right)^2\right]}{\left[\left(1-\upsilon_c\right)+\left(1+\upsilon_c\right)\left(a/R\right)^2\right]} \quad (4)$$

Where a is the radius of the indentation and R is the radius of the annular interface generated when spalling occurs.

The circumferential strain (ε_θ) and radial strain (ε_r) can be calculated using a model that surrounds the indenter contact in a semi-spherical cavity, where a hydrostatic stress exists inside the cavity [16]. The limit between the elastic and the plastic zones is defined by a radius c given by:

$$c = a\left[\frac{E^*\tan\beta/\sigma_{Ys}+4\left(1-2\upsilon_s\right)}{6\left(1-\upsilon_s\right)}\right]^{1/3} \quad (5)$$

Where β is the angle between the indenter and the surface, σ_{Ys} is the substrate yield stress, υ_s is the substrate Poisson coefficient, and E* is the combined Young´s modulus.

According to Xie and Hawthorne [17], if the crack is located within the plastic region (a≤R≤c), then the surface radial strain is given by Eq. 6; if the crack is within the elastic region (c≤R), then it is given by Eq. 7:

$$\varepsilon_r\left(R\right) = -\frac{\sigma_{Ys}}{E^*}\left[6\left(1-2\upsilon_s\right)\ln\frac{c}{R}+\frac{2}{3}\left(1+\upsilon_s\right)\left(\frac{c}{R}\right)^3\right] \quad (6)$$

$$\varepsilon_r\left(R\right) = -\frac{2}{3}\frac{\sigma_{Ys}}{E^*}\left(1+\upsilon_s\right)\left(\frac{c}{R}\right)^3 \quad (7)$$

And the circumferential strain is given by:

$$\varepsilon_\theta(R) = \frac{\sigma_{Ys}}{3E^*}(1+\upsilon_s)\left(\frac{c}{R}\right)^3 \quad (8)$$

Therefore, if the extent of the spalling is measured and substituted as the radius of the annular interface produced by indentation in Eq. 1 to 8, the interface adhesion Γ_c can be calculated.

2.3. Parameters of the indentation and the annular interface.

The indentation tests used a Rockwell C indenter under normal loads of 10, 20, 30, 50, 100, 200, 400, 1000, and 1500N and the same indentation tests were simulated using FilmDoctor®. A Young´s modulus of 1141 GPa and a Poisson coefficient of 0.07 were set for the diamond indenter [11].

DLC spalling during indentation tests is shown in Fig. 3 for situations where total spalling occurred (Fig. 3.a) and for partial spalling conditions (Fig. 3.b). The extent of the spalling was measured from SEM and laser interferometry images (Fig. 4).

Because spalling occurred due to shear stresses, the interface fracture toughness (K_{IIC}) was calculated using Eq 9 [18].

$$G_t = \frac{1}{2}\left(1-\beta_d^{\,2}\right)\left[\frac{1-\upsilon_1^2}{E_1}+\frac{1-\upsilon_2^2}{E_2}\right]K_{IIC}^2 \quad (9)$$

Where E and υ are Young´s modulus and the Poisson coefficient, respectively, of the two adjacent layers that compose the interface, with indices 1 and 2, and β_d is Dundurs' parameter [18], defined as:

$$\beta_d = \frac{1}{2}\frac{\mu_1(1-2\upsilon_2)-\mu_2(1-2\upsilon_1)}{\mu_1(1-\upsilon_2)+\mu_2(1-\upsilon_1)} \quad (10)$$

Where

$$\mu_i = \frac{0{,}5E_i}{(1+\upsilon_i)} \quad (11)$$

The critical stresses at the interface between CrN and DLC (interface critical stress) were determined through indentation tests. For a given crack length (a_c) and an interface fracture toughness (K_{IIC}), the interface critical stresses (σ_c) were calculated using Eq. 12.

$$\sigma_C = \frac{K_{IIC}}{\sqrt{\pi a_c}} \quad (12)$$

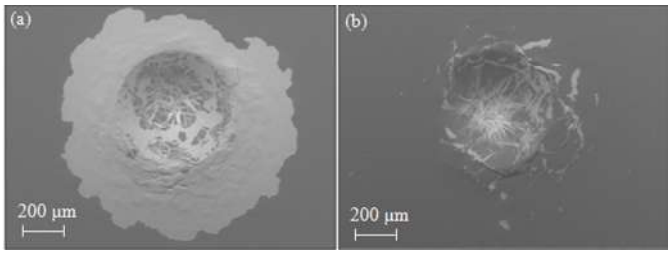

Figure 3. DLC spalling for an indentation load of 400 N: (a) Sample B; (b) Sample C.

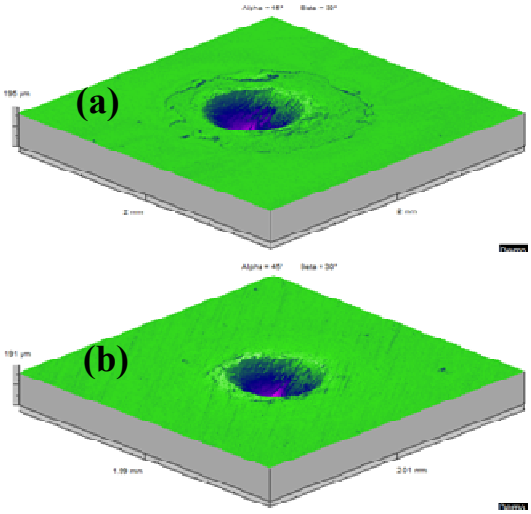

Figure 4. Laser interferometry images of DLC spalling for an indentation load of 400 N: (a) Sample B; (b) Sample C.

To analyse the effect of the film thickness on stress distributions on the coated systems, the results from indentation tests were compared to the shear stresses at the simulated interfaces (interface shear stress). The simulation tests used the commercial software FilmDoctor®.

3. RESULTS AND DISCUSSIONS

In this experiment, three one-coating specimens were used and three indentations were made for each load on each specimen. Figure 5 shows the compositional maps obtained by EDX. The elements C and Cr in the sample indicate that all spalling occurred in the interface between CrN and DLC.

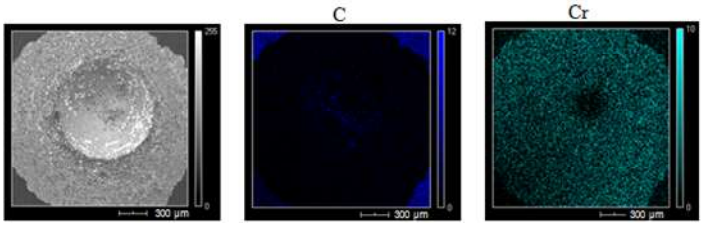

Figure 5. Compositional maps of the elements C and Cr.

Figure 6 shows the adhesion at the DLC/CrN interface, given by Eq. 2.

The adhesion values at the DLC/CrN interface and the interface fracture toughnesses are higher for sample C, which is the sample with the thinner coating, and are lower for samples A and B, which represent the samples with thicker coatings.

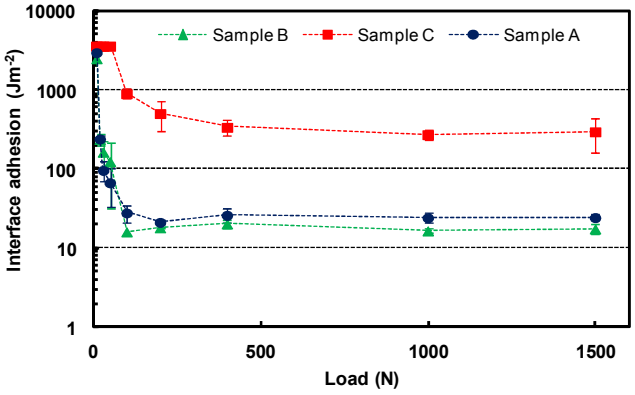

Figure 6. Interface adhesion.

Figure 6 shows the adhesion at the DLC/CrN interface, given by Eq. 2.

The adhesion at the DLC/CrN interfaces for samples A, B and C are 25.04 ± 2.51 Jm^{-2}, 17.88 ± 1.65 Jm^{-2} and 305.90 ± 33.46 Jm^{-2}, respectively.

Using Eq. 9, the value of the interface fracture toughness between CrN and DLC is determined, as shown in Fig. 7.

The fracture toughness at the DLC/CrN interfaces for samples A, B and C are 1.59 ± 0.08 MPam$^{1/2}$, 1.23 ± 0.06 MPam$^{1/2}$ and 8.43 ± 0.46 MPam$^{1/2}$, respectively.

Figures 8 and 9 compare the critical stresses at the interface between CrN and DLC (interface critical stress) and the shear stresses at the interfaces calculated by the simulations (interface shear stress).

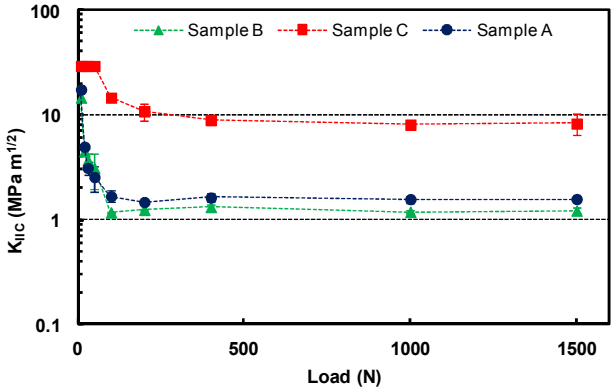

Figure 7. Interface fracture toughness.

Spalling is expected to occur when the interface shear stress reaches the critical stress at the interface, i.e., for the load value where the blue and red curves intercept. For sample C, the critical stress at the interface is reached for loads between 50 and 100 N. For samples A and B, this intercept occurs between 10 and 20 N, i.e., spalling should occur for substantially lower loads.

The thinner films (sample C) are subjected to higher interface shear stresses (blue curves) than the thicker films (samples A and B), according to the results from the simulations.

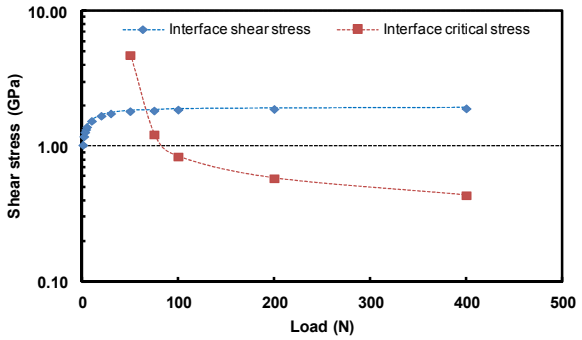

Figure 8. Example of critical interfacial stresses, obtained experimentally, and shear stresses at the interface, calculated by simulations, for the thinner coatings on sample C.

The adhesion values at the DLC/CrN interface and the interface fracture toughnesses are higher for sample C, which is the sample with the thinner coating, and are lower for samples A and B, which represent the samples with thicker coatings interface, calculated by simulations, for the thicker coatings on samples A and B.

Sample C, which represents the thinner coatings, is subjected to higher interface shear stresses than the thicker films (samples A and B), as shown in the simulation. Its critical stresses at the interface, made through indentation tests, are higher than the critical stresses at the interface of the thicker films.

In this paper, the determination of the radius of the annular interface accounts for the occurrence of the spalling. However, the calculations do not consider whether this occurs wholly or partially. In this work, all spalling of sample C was partial spalling.

4. CONCLUSIONS

The thinner film (sample C) has a higher interface adhesion and interface fracture toughness than the thicker films (samples A and B). The highest critical loads were found on the thinner film and coating thicknesses have an important role in the interface adhesion of the coated systems.

5. REFERENCES

[1] C. Donnet, A. Erdemir, Historical Developments and New Trends in Tribological and Solid Lubricant Coatings, *Surf. Coat. Technol*., 180–181, 76–84, **2004**.

[2] J.D.B. De Mello, R. Binder, A Methodology to Determine Surface Durability in Multifunctional Coatings Applied to Soft Substrates, *Tribol. Int*., 39, 769–773, **2006**.

[3] K.J. Ma, A. Bloyce, T. Bell, Examination of mechanical properties and failure mechanisms of TiN and Ti-TiN multilayer coatings, *Surface and Coat Technology*, 76–77, 297, **1995**.

[4] H. Zaidi, A. Djamai, K.J. Chin, T. Mathia, Characterisation of DLC Coating Adherence by Scratch Testing, *Tribology International*, 39, 124–128, **2006**.

[5] N. Schwarzer, M. Fuchs, Comprehensive Analysis Of Thin Film Nanoindentation Data Via Internetportal - A Principal Feasibility Study, *Thin Solid Films*, 515, 1080–1086, **2006**.

[6] N. Schwarzer, The Extended Hertzian Theory and its Uses in Analyzing Indentation Experiments, *Philosophical Magazine*, 86, 33-35, **2006**.

[7] N. Schwarzer; L. Geidel, Automated Analysing of Thin Film Nanoindentation Data Using the Concept of the Effectively Shaped Indenter, *Surface & Coatings Technology*, 201, 4377–4383, **2006**.

[8] A. Bolshakov, W.C. Oliver, G.M. Pharr, An explanation for the shape of nanoindentation unloading curves based on finite element simulation, in: S.P. Baker, C.A. Ross, P.H. Townsend, C.A. Volkert, P. Borgesen (Eds.) Thin Films: Stresses and Mechanical Properties V, *Materials Research Soc*, Pittsburgh, 675-680, **1995**.

[9] L.O.C. Lara, J.D.B.d. Mello, Influence of layer thickness on hardness and scratch resistance of Si-DLC/CrN coatings. Tribology (Leeds. Print)., 6, 168 - 173, **2012**.

[10] L.O.C. Lara, J.D.B.d. Mello, Efeito da espessura de camadas na dureza instrumentada de revestimentos multifuncionais, in: ABM (Ed.) 61th Internacional ABM Congress, Rio de Janeiro, 4185-4196, **2012**.

[11] W.C. Oliver, G.M. Pharr, An Improved Technique for Determining Hardness and Elastic Modulus Using Load and Displacement Sensing Indentation Experiments, *Journal of Materials Research*, 7, 6, 1564, **1992**.

[12] N. Schwarzer, About The Characterization of Ultra Thin Coatings via Nanoindenter, publication of the Saxonian Institute of Surface Mechanics, online at www.siomec.de/doc/**2007**.

[13] Y. Xie, H.M. Hawthorne, Measuring The Adhesion of Sol–Gel Derived Coatings to a Ductile Substrate by an Indentation-

Based Method, *Surface and Coatings Technology*, 172, 42–50, **2003**.
[14] Y. Xie, X. Zhang, M. Robertson, R. Maric, D. Ghosh, Measurement of The Interface Adhesion of Solid Oxide Fuel Cells by Indentation, *Journal of Power Sources*, 162, 436–443, **2006**.
[15] M.D. Drory, J.W. Hutchinson, Measurement of The Adhesion of a Brittle Film on a Ductile Substrate by Indentation, *Proc. R. Soc. Lond*., A 452, 2319–2341, **1996**.
[16] K.L. Johnson, *Contact Mechanics*, Cambridge University Press, Cambridge, UK, **1985**.
[17] Y. Xie, H.M. Hawthorne, A Model for Compressive Coating Stresses in the Scratch Adhesion Test, *Surface and Coatings Technology*, 141, 15–25, **2001**.
[18] V. Tvergaard, J.W. Hutchinson, The Influence of Plasticity on Mixed Mode Interface Toughness, *Journal of the Mechanics and Physics of Solids*, 41, 1119-1135, **1993**.

6. ACKNOWLEDGEMENTS

The authors are very grateful to Fapemig, Capes/Proex and CNPq (Brazil) for financial support.